Binding mode dependent signaling for the detection of Cu2+: An experimental and theoretical approach with practical applications

Soumen Ghosh, Mehebub Ali Khan, Aniruddha Ganguly, Abdulla Al Masum, Md. Akhtarul Alam, Nikhil Guchhait

PII: S1386-1425(17)30776-X
DOI: doi: 10.1016/j.saa.2017.09.049
Reference: SAA 15483

To appear in: *Spectrochimica Acta Part A: Molecular and Biomolecular Spectroscopy*

Received date: 18 February 2017
Revised date: 14 September 2017
Accepted date: 16 September 2017

Please cite this article as: Soumen Ghosh, Mehebub Ali Khan, Aniruddha Ganguly, Abdulla Al Masum, Md. Akhtarul Alam, Nikhil Guchhait , Binding mode dependent signaling for the detection of Cu2+: An experimental and theoretical approach with practical applications, *Spectrochimica Acta Part A: Molecular and Biomolecular Spectroscopy* (2017), doi: 10.1016/j.saa.2017.09.049

Binding mode dependent signaling for the detection of Cu^{2+}: An experimental and theoretical approach with practical applications

Soumen Ghosh[a], Mehebub Ali Khan[b], Aniruddha Ganguly[a], Abdulla Al Masum[b], Md. Akhtarul Alam[b*] and Nikhil Guchhait[a*]

[a]Department of Chemistry

University of Calcutta

92, A.P.C. Road, Kolkata 700 009, India

Telephone 91-33-23508386

Fax: 91-33-23519755

[b]Department of Chemistry

Aliah University

IIA/27, New Town, Kolkata-700 156, West Bengal, India

[*]Corresponding author, E-mail:alam_iitg@yahoo.com

Corresponding author, E-mail: nguchhait@yahoo.com (N.G.)

Abstract

Two amido-schiff bases (3-Hydroxy-naphthalene-2-carboxylic acid pyren-1-ylmethylene-hydrazide and Naphthalene-2-carboxylic acid pyren-1-ylmethylene-hydrazide) have been synthesized having a common structural unit and only differs by a –OH group in the naphthalene ring. Both of them can detect Cu^{2+} ion selectively in semi-aqueous medium in distinctly different output modes (one detects Cu^{2+} by naked-eye color change where as the other detects Cu^{2+} by fluorescence enhancement). The difference in the binding of Cu^{2+} with the compounds is the reason for this observation. The detection limit is found to be micromolar region for compound which contains –OH group whereas the compound without –OH group detects copper in nano-molar region. DFT calculations have been performed in order to demonstrate the structure of the compounds and their copper complexes. Practical utility has been explored by successful paper strip response of both the compounds. The biological applications have been evaluated in RAW 264.7.

Key Words: Colorimetric sensing, Fluorescence enhancement, Ion detection, Schiff base, LMCT, Test Kit

1. Introduction

Copper is the third abundant ion among the essential transition metal ions in the human body being involved in various important physiological processes [1]. However, excess intake of copper exhibits toxicity, causing serious neurodegenerative diseases, such as Menkes, Alzheimer's and Wilson's diseases due to displacement of other vital metal ions in enzyme-catalyzed reactions [2]. On the other hand, a deficiency of copper has effects on neuro-behavior and the immune system, abnormal glucose and cholesterol metabolism [3]. Thus, development of biologically compatible sensors selective for detecting copper ion is necessary and indispensable for environmental protection and human health. Up to now various methods, such as electrochemical, atomic absorption spectroscopy, UV-Vis absorption spectroscopy, fluorescence spectroscopy and colorimetry have been employed to measure trace amount of copper ions [4,10]. With comparison to other techniques, colorimetric and fluorometric techniques are the most promising tool for the detection of metal ions due to their high sensitivity, instantaneous response and cost-effectiveness [11,12]. In colorimetric technique, the sensor molecule immediately changes its color in presence of guest ions and in fluoremetric technique the sensor molecule shows instantaneous ion-induced change of emission signal. Both colorimetric and fluorometric sensors are composed of a metal binding unit and a signaling unit. But there are some problems regarding both the aforesaid methods for the sensing of Cu^{2+} [13,14]. In case of colorimetric sensing sometimes other metal ions like iron, mercury, aluminium interfere by exhibiting same color where as Cu^{2+} is known as a fluorescence quencher [15,16]. Due to these problems, design and synthesis of new molecules capable of sensing Cu^{2+} selectively by both colorimetrically and fluorometrically is an interesting research area till now. A numbers of Cu^{2+} ion sensors have been reported in the literature by several groups, but a few of them show their

interest to investigate the effect of mode of binding of Cu^{2+} with the ligands on the signaling property of the ligands [17,18]. In the present study, two pyrene-based sensors (**1** and **2**) have been synthesized for Cu^{2+} detection. It is noteworthy to mention that the basic framework of sensors **1** and **2** is same, only differs by a –OH group. Compound **1** contain a –OH group in the naphthalene ring which is absent in compound **2**. Between these two sensors, **1** detects Cu^{2+} colorimetrically (light yellow to brown) and **2** fluorometrically (fluorescence enhancement) depending on their binding modes in semi aqueous medium. Furthermore, practical applications (like test-kit, live cell imaging) of **1** and **2** have been performed to ensure their real time acceptability.

2. Experimental

2.1. Instrumentation

Electronic absorption spectra, fluorescence spectra and fluorescence lifetime have been recorded by a Hitachi UV-Vis (Model U–3501), Perkin Elmer LS-55 spectrofluorimeter and Time Correlated Single Photon Counting (TCSPC) spectrophotometer (Horiba Jobin Yovin) respectively. IR spectra (KBr pellet, 4000–400 cm^{-1}) have been recorded on a Parkin Elmer modal 883 infrared spectrophotometer. ^1H NMR spectra have been recorded on a Bruker, Avance 300 spectrometer, where chemical shifts (δ in ppm) have been determined with respect to tetramethylsilane (TMS) as internal standards. Mass spectrum was recorded on Waters Xevo G2-S Q TOF mass spectrometer.

2.2. Reagents

All reagents and solvents have been used as received from commercial sources without further purification. All cations in the form of perchlorate salts have been purchased from Sigma-Aldrich Chemical Company. All solvents used for the spectroscopic studies are spectroscopic grade. Here all the spectroscopic experiments have been done in methanol-water mixture (CH_3OH:H_2O = 7:3, v/v, pH=7.2). The pH of this mixture has been maintained using Tris-HCl buffer.

2.3. Cell Culture. Abelson murine leukemia virus-induced tumor cells RAW 264.7 have been obtained from National Institute of Cell Science (NCCS), Pune, India. Cells have been grown by continuous culture in Dulbecco's Modified Eagle's Medium (DMEM, Sigma Chemical Co., St. Louis, MO) supplemented with 10% fetal bovine serum (Invitrogen), penicillin/streptomycin (100 units/ml) and antibiotics in a CO_2 incubator. The cells initially propagates in 75 cm^2 polystyrene, filter-capped tissue culture flask in an atmosphere of 5% CO_2 and 95% air at 37°C in CO_2 incubator. When the cells reach the logarithmic phase, the cell density has been adjusted to 1.0 x 10^5 per/well in culture media. The cells have been used to inoculate in a glass bottom dish, with 1.0 mL (1.0 x 10^4 cells) of cell suspension in each dish. After cell adhesion, culture medium has been removed. The cell layer has been rinsed twice with phosphate buffered saline (PBS), and then treated according to the experimental need.

2.4. Cell Imaging Study. For fluorescence microscopic studies, RAW264.7 cells in 1000 μL of medium, have been seeded on sterile 35 mm glass bottom culture dish (ibidi GmbH, Germany), and incubated at 37 °C in a CO_2 incubator for 10 hours. Then cells have been washed with 500 μL DMEM followed by incubation with 1.0 x 10^{-6} M solution of compound **2** dissolved in 1000 μL DMEM at 37°C for 1 h in a CO_2 incubator and observed under a fluorescence

microscope (Leica) at different time interval. Then the cells have been washed four times with phosphate buffered saline PBS (pH 7.4) to remove any free compound **2** outside the cells and incubated in PBS containing metal $\mathbf{Cu^{2+}}$ to a final concentrations of 1.0 x 10^{-4} M, incubated for 20 min followed by washing with PBS three times to remove excess metal outside the cells and images were captured.

2.5. Syntheses

The compound 3-hydroxy-naphthalene-2-carboxylic acid hydrazide has been synthesized from 3-hydroxy-naphthalene-2-carboxylic acid ethyl ester accroding to the literature procedure [19,20].

2.5.1. Compound 1: Sythesis of *3-Hydroxy-naphthalene-2-carboxylic acid pyren-1-ylmethylene-hydrazide* **(compound 1)**

Compound 3-hydroxy-naphthalene-2-carboxylic acid hydrazide (1.5 mmol, 0.30 g) has been treated with 1-pyrene carboxaldehyde (1.5 mmol, 0.20 g) in methanol at 50 ^{o}C for 2 hrs. to form a yellow solid. The product thus obtained has been filtered and then dried under vacuum (yield: 0.35 g, 76%). ^{1}H NMR (Fig. S1) in d_6-DMSO, 300MHz, δ (ppm): 12.21 (s, 1H, –CONH–), 11.40 (s, 1H, –OH), 9.54 (s, 1H, –CH=N–), 9.54 (d,1H), –), 8.93 (d, J=12.3 Hz,1H), 8.88 (s, 1H), 8.64-7.78 (m, 9H), 7.56-7.39 (m, 3H). ^{13}C NMR (Fig. S2) (75.5 MHz, d_6-DMSO, 20 ºC) δ (ppm): 110.37, 119.97, 122.31, 123.42, 123.62, 123.82, 124.93,125.54, 125.87, 126.35, 126.46, 126.55, 127.09, 128.07, 128.26, 128.52, 129.82, 130.10, 130.51, 131.81, 135.62, 147.14, 153.72, 163.58. IR (KBr): 3399, 3222, 3093, 1649, 1620, 1597, 1541, 1507, 1219 cm^{-1}. Mass (TOF-MS ES+) m/z: calcd. for $C_{28}H_{18}N_2O_2$ $[M+H]^+$, 415.14; found, 415.139. $[M+Na]^+$, 415.14; found,

437.12. Elemental analysis calculated for $C_{28}H_{18}N_2O_2$: C, 81.14; H, 4.38; N, 6.76. Found: C, 80.93; H, 4.32; N, 6.84.

2.5.2. Compound 2: Sythesis of *Naphthalene-2-carboxylic acid pyren-1-ylmethylene-hydrazide* **(compound 2)**

Compound **2** has been prepared according to the similar procedure as compound **1** by the reaction between naphthalene-2-carboxylic acid hydrazide (1.3 mmol, 0.250 g) and 1-pyrene carboxaldehyde (1.4 mmol, 0.180 g) in methanol. The yellow solid thus obtained was filtered and then dried under vacuum (yield: 0.32 g, 80%). ^{1}H NMR (Fig. S3) in d_6-DMSO, 300MHz, δ (ppm): 12.24 (s, 1H, –CONH–), 9.57 (s, 1H, –CH=N–), 8.61 (d, J=8.5 Hz, 1H), 8.39-8.35 (m, 2H), 8.26-8.08 (m, 11H), 7.65-7.64 (m, 2H) ^{13}C NMR (Fig. S4) (75.5 MHz, d_6-DMSO, 20 ºC) δ (ppm): 121.91, 123.26, 123.64, 123.76, 124.56, 124.74, 125.26, 125.60, 126.10, 126.45, 126.89, 127.20, 127.48, 127.71, 127.90, 128.26, 128.39, 129.62, 130.34, 131.43, 131.60, 133.88, 146.09, 163. IR (KBr): 3428, 3205, 3050, 2924, 2852, 1635, 1625, 1593, 1543, 1301 cm^{-1}. Mass (TOF-MS ES+) m/z: calcd. for $C_{28}H_{18}N_2O$ $[M+H]^+$, 399.14; found, 399.14. $[M+Na]^+$, 421.13; found, 421.13. Elemental analysis calculated for $C_{28}H_{18}N_2O$: C, 84.40; H, 4.55; N, 7.03. Found: C, 84.47; H, 4.51; N, 6.96.

3. Results and discussion

The compounds **1** and **2** have been synthesized following two steps. Firstly, acid hydrazides have been prepared by the reaction of hydrazine with the corresponding ethyl ester derivatives then they have been condensed with pyrene-1-carboxaldehyde (Scheme 1). The compounds **1** and **2** have been characterized by ^{1}H, ^{13}C NMR (Fig. S1-S4) and IR spectroscopic methods. The FT-IR

spectroscopy suggests the presence of two functional groups amido (–CONH–) and imino (–CH=N–) group by the absorption peaks in the range of 1649 to 1620 cm^{-1} [21]. In ^{1}H-NMR spectra, the presence of (–CONH–) and imino (–CH=N–) groups have been confirmed by their two characteristic peaks at 12.2 ppm and 9.5 ppm respectively.

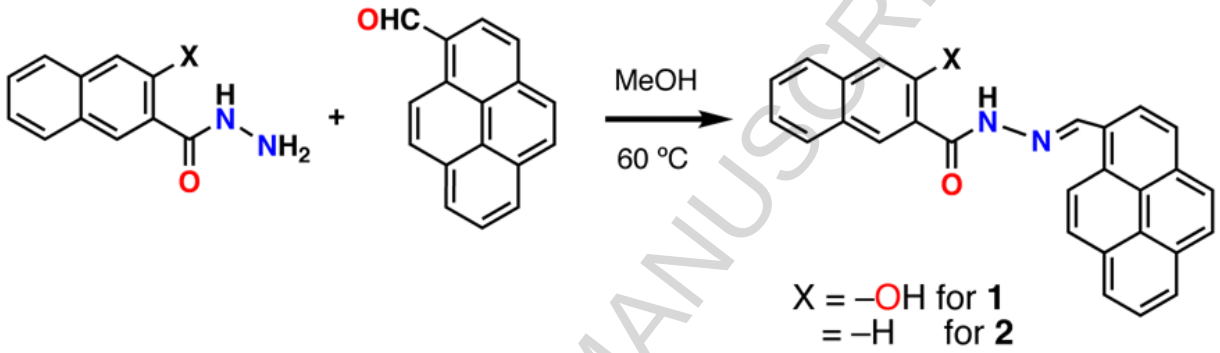

Scheme 1: Synthetic procedure of compound **1** and **2**.

3.1. Naked-eye sensing of cations

According to the literature reports compounds having amide or phenolic –OH groups have certain affinity towards cations. Keeping this fact in mind, colorimetric sensing ability of compound **1** and **2** (10^{-4} M) towards cations has been investigated in aqueous methanolic medium (methanol: water = 7:3, v/v). When methanolic solution of all cations (such as Fe^{3+}, Co^{2+}, Ni^{2+}, Cu^{2+}, Zn^{2+}, Cd^{2+}, Fe^{2+}, Hg^{2+} and Mn^{2+}) have been added seperately to the solutions of **1**, only Cu^{2+} shows a distinct color change from light yellow to brown whereas some of the other

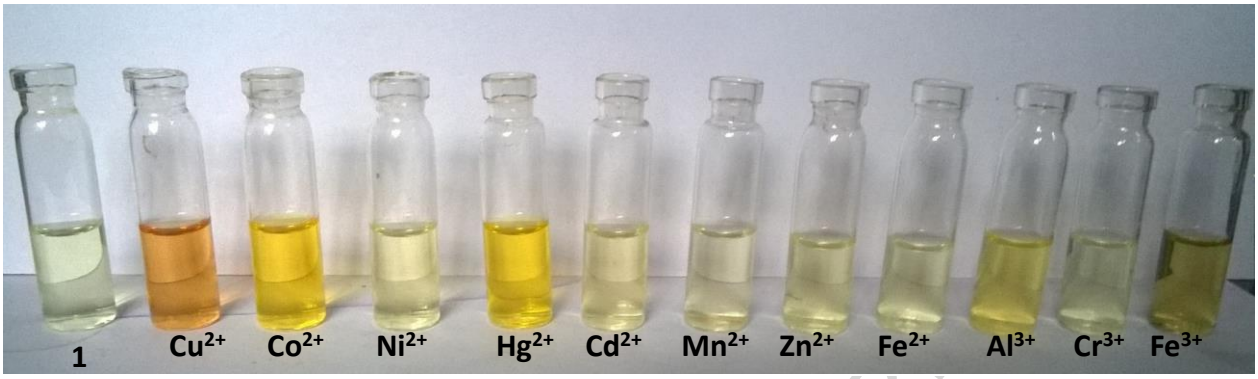

Fig. 1. Naked-eye color changes of compound **1** (1.0×10^{-5} M) after addition of 2 equivalent of various cations (1.0×10^{-4}) M in methanol water mixture ($CH_3OH–H_2O$ = 7:3, v/v).

cations (such as Co^{2+}, Hg^{2+}, Al^{3+} and Fe^{3+}) show intensification of the color of compound **1** (Fig. 1). Under same experimental condition compound **2** does not show any notable color change (ESI, Fig. S5). This indicats that compound **1** can serve as a potential candidate for the detection of Cu^{2+} ion colorimetrically in semi aqueous medium.

3.2. UV-Vis spectroscopic experiment

The sensing ability of compound **1** and **2 (**10^{-6} M) has also been monitored by UV-Vis spectroscopy in aqueous methanolic solution (methanol: water = 7:3, v/v). Compound **1** exhibits mainly two absorption bands at 289 nm and 379 nm with a hump at 401 nm in aqueous methanolic solution. On sequential addition of Cu^{2+} to the aqueous methanolic solution of **1** a new broad band appears near 485 nm with gradual decreament of the band at 379 nm, resulting in a color change from light yellow to brown (Fig. 2). Under same condition all other cations remain almost inert except Co^{2+}, Hg^{2+}, Al^{3+} and Fe^{3+} which give slight modification of the

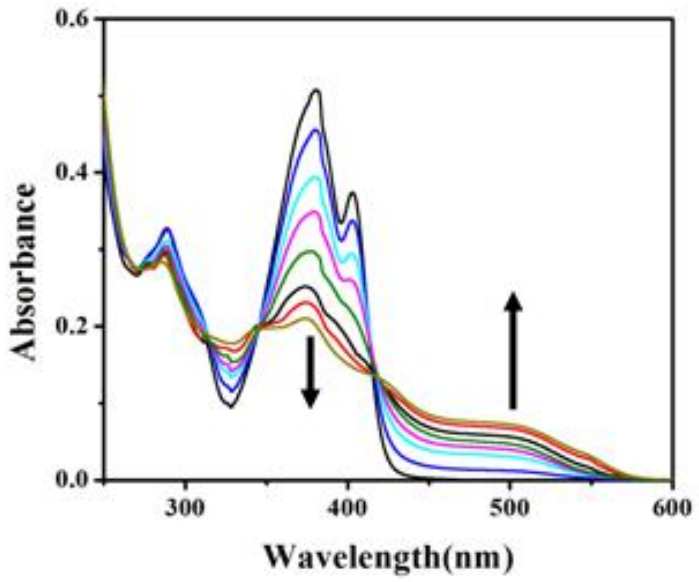

Fig. 2.UV–Vis spectral changes of compound **1** (1.0×10^{-6} M) upon addition of Cu^{2+} ion (0–5 equiv.) in methanol water mixture ($CH_3OH–H_2O$ = 7:3, v/v)

absorption spectra of compound **1** (ESI, Fig. S6). On the other hand compound **2** shows two absorption bands at 283 nm and 372 nm with a hump at 398 nm in aqueous methanolic solution. The UV-Vis spectra of compound **2** remain almost uneffected in presence of the aforesaid cations (ESI, Fig. S7). Now to find out the selectivity of **1** (1μM) towards Cu^{2+} (5μM), UV-Vis study has been performed in aqueous methanolic solution (methanol:water = 7: 3) in presence of other competing metal ions (5μM). This experiment shows compound **1** exhibits almost same optical density in presence of other competitive metal ions (ESI Fig. S8a and Fig. S8b), indicating the selectivity of **1** towards Cu^{2+} ion having a detection limit of 2.3 x 10^{-6} M (ESI Fig. S9). The effect of pH on the sensing behavior of **1** has also been checked. It has been found that

compound **1** shows good response towards Cu^{2+} in the pH range from 5 to 8 (ESI Fig. S10a). To understand the stability and reversibility of the **1**- Cu^{2+} complex, ethylenediaminetetraacetic acid (EDTA)-addition experiments have been performed in methanol water mixture. After adding 6 equiv of EDTA to 1-Cu^{2+} solution, the color of the solution changes from brown to light yellow and the absorbance at 485 nm completely is found to be changed. Upon addition of Cu^{2+} into that solution again, the color and the absorbance is recovered. The color change (Fig. S10b) and absorbance (Fig. S10b) are almost reversible even after several cycles with the sequentially alternative addition of Cu^{2+} and EDTA.

3.3. Spectrofluorometric experiment

The fluorescence properties of both **1** and **2 (**10^{-7} M) have been investigated upon addition of various metal ions like $Fe^{3+,}$ Al^{3+}, Cr^{3+}, Co^{2+}, Ni^{2+}, Cu^{2+}, Zn^{2+}, Cd^{2+}, Fe^{2+}, Hg^{2+} and Mn^{2+} in aqueous methanolic solution (methanol: water = 7:3, v/v). Surprisingly compound **1** shows very little fluorescence change towards the above mentioned cations where as compound **2** shows massive fluorescence enhancement in presence of Cu^{2+} (ESI, Fig. S11 and Fig. S12). On addition of methanolic solution of Cu^{2+} to the aqueous methanolic solution of compound **2** the fluorescence intensity is found to increase in the region 410 nm to 460 nm which finally resolves into two bands at 414 nm and 432 nm (Fig. 3). Interestingly, under UV light the

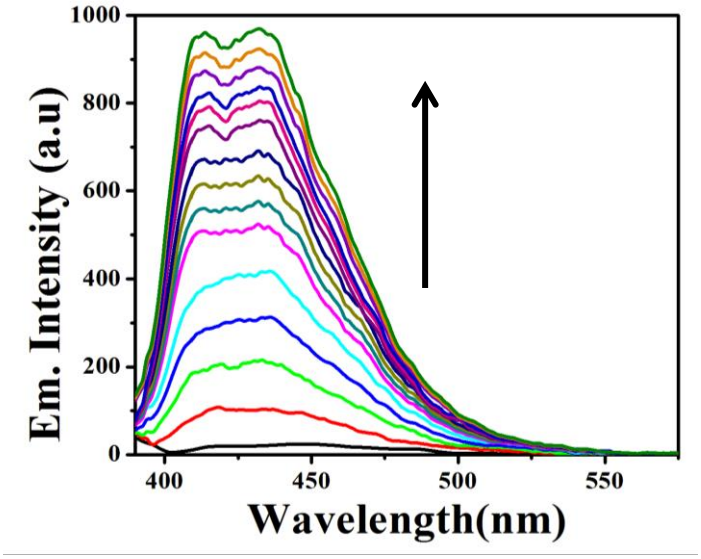

Fig. 3. Fluorescence (λ_{ex}= 375 nm) spectral changes of **2** (1.0×10^{-7} M) upon addition of Cu^{2+} ion (0–5 equiv) methanol water mixture ($CH_3OH–H_2O$ = 7:3, v/v).

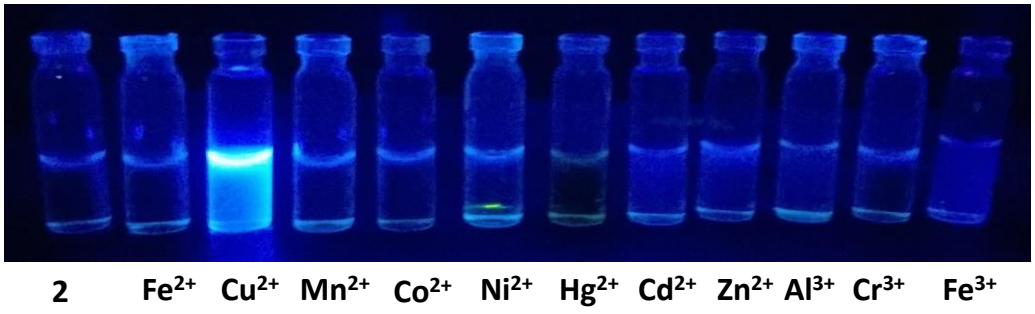

Fig. 4. The color change of **2**(1.0×10^{-6} M) in methanol water mixture ($CH_3OH–H_2O$ = 7:3, v/v) without and with addition of various cations (1.0×10^{-5} M) under UV light.

aqueous methanolic solution of **2** has no such noticeable fluorescence, whereas in presence of Cu^{2+} a bluish white colored fluorescence has been observed in methanol water mixture (Fig. 4). From the above two experiments it can be said that compound **2** can detect Cu^{2+} in aqueous methanolic mixture. To understand the selectivity of compound **2** toward Cu^{2+} over other metals, the competition experiments have been performed using the method of the fluorescence. The fluorescence spectra of compound **2** (0.1μM) has been recorded on addition of 1μM Cu^{2+} to the mixture of **2** and 1 μM of other interfering metal ions Mg^{2+}, $Ca^{2+,}$ Cr^{3+}, Ni^{2+}, Zn^{2+}, Co^{2+}, Cd^{2+}, Hg^{2+}, Fe^{2+} and Pb^{2+} (ESI Fig. S12b) and visual fluorescence change of compound **2** (1μM) has also monitored in presence of cation mixture (S12b, inset). These experiments indicate high selectivity of compound 2 towards Cu^{2+} which has been furnished in the form of bar plot (S13). The detection limit of compond **2** towards Cu^{2+}has been found to be 4.1nM (ESI, Fig. S14). The fluorescence intensity of **2** in the presence and absence of Cu^{2+} at various pH values has also been monitored. It has been found that in the absence of Cu^{2+}, the fluorescence intensity of **2** does not changes noticeable. When Cu^{2+} has been added compound **2** shows appreciable fluorescence enhancement in the pH range from 4.5 to 9 (ESI, Fig. S15a). Again, to check the reversibility of the **2**- Cu^{2+} complex, ethylenediaminetetraacetic acid (EDTA)-addition experiments have been performed in methanol water mixture. This experiment shows that the fluorescence change (Fig. S15b) is almost reversible even after several cycles with the sequentially alternative addition of Cu^{2+} and EDTA.

3.4. Fluorescence quantum yield

The fluorescence quantum yields have been determined using quinine sulfate as the secondary standard (Φ_R = 0.54 in 0.1 M H_2SO_4). The area of the emission spectrum is integrated using the software available in the instrument and the quantum yield is calculated according to the following equation:

$$\Phi_S/\Phi_R = [A_S/A_R] \times [(Abs)_R/(Abs)_S] \times [\eta_S^2/\eta_R^2]$$

where Φ_S and Φ_R are the fluorescence quantum yield of the sample and reference, respectively; A_S and A_R are the area under the fluorescence spectra of the sample and the reference, respectively; $(Abs)_S$ and $(Abs)_R$ are the corresponding optical densities of the sample and the reference solution at the wavelength of excitation; η_S and η_R are the refractive index of the sample and the reference, respectively. The quantum yield of compound **1** is 0.023 where as with the addition of Cu^{2+} the quantum yield is 0.091. The quantum yield of compound **2** is 0.052 and the quantum yield of the **2**-Cu^{2+} complex is 0.54.

3.5. Fluorescence lifetime measurements

Fluorescence decay analysis of the fluorophore gives the informations about its local environment and its excited state behaviour. Fluorescence lifetime measurements of compound **2** have been done in methanol water mixture at λ_{ex}=375 nm. The decay profile of **2** shows that the fluorescence lifetime of **2** is very short which undergoes a drastic modification with the addition of Cu^{2+} indicating a strong interaction of **2** with Cu^{2+} (Fig. 5, ESI Table S1). The fluorescence lifetime data shows that the average lifetime of **2** increases to a huge extent in presence of Cu^{2+}. This can be attributed to the formation of comparatively rigid structure imposed on the compound **2** by strong complexation with Cu^{2+} ion. Rigid structural architecture of **2** in the complex restricts free motion of flexible bonds and there by minimizes the radiationless transition, consequently excited state lifetime increases [22-23].

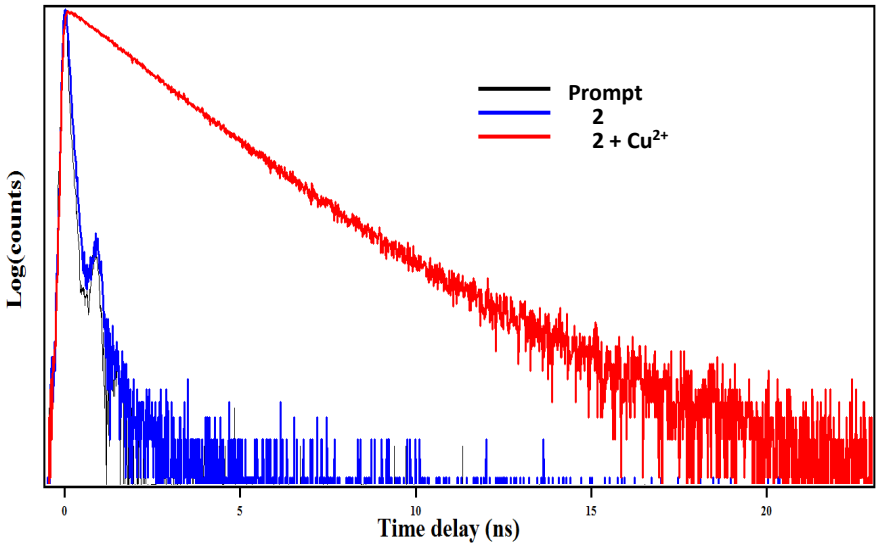

Fig. 5. Fluorescence decay profile of **2** in presence of 2 equivalents of Cu^{2+}, λ_{ex} = 375 nm, $\lambda_{em\ (max)}$ = 430 nm.

3.6. Elucidation of binding mechanism

The mechanism behind this unanticipated phenomenon, compound **1** detects Cu^{2+} by naked-eye color change /UV-Vis experiment where as compound **2** detects Cu^{2+} via fluorescence enhancement, is no doubt very interesting. These phenomenons can be explained by considering the binding mode of Cu^{2+} with the ligands. Compound **1** can bind with Cu^{2+} in two possible ways, one is the binding of Cu^{2+} with phenolic oxygen and amide oxygen of the ligand to form a six membered ring and another is a five membered ring formed by the complexation between Cu^{2+} with the oxygen of the amide and the immine nitrogen, but the more stable six membered ring will be the obvious choice (ESI, Fig. S16). As a result both the phenolic –OH group gets deprotonated which may cause a ligand to metal charge transfer from **1** to Cu^{2+} resulting a color change from light yellow to brown [24-26]. IR spectra also indicates that -CONH- group and-OH group take part in

complexation whereas azomethine group (-CH=N-) does not participate (ESI, Fig. S17 and Table S2). But this type of binding cannot give enough structural rigidity to the main fluorophore unit (pyrene) to show fluorescence enhancement. In case of compound **2** there is only one binding site which is the five membered ring formed by the complexation between the oxygen of the amide, the immine nitrogen and Cu^{2+} (ESI, Fig. S18, S19 and Table S2). This mode of binding somehow gives adequate structural rigidity to the fluorophore unit [27]. Now, in order to understand the binding stoichiometry of both the two complexes, Job's plot has been done. Interestingly both the complexes show 2:1 (ligand:metal) complexation (ESI, Fig. S20a and Fig. S20b). To confirm the stoichiometry of [**1**–Cu^{2+}] and [**2**–Cu^{2+}] complexes mass spectral analysis of those complexes have been done. For this purpose those complexes has been synthesized by the reaction between the ligands (1eq.) with copper perchlorate (1eq.) in methanol. In case of [**1**-Cu^{2+}] complex the peak in mass spectra at 921.95 confirms 2:1 complexation between **1** and Cu^{2+} with one methanol as coordinating solvent (ESI, Fig. S21, left). On the other hand, the presence of the peak at 860.22 in the mass spectra of [**2**-Cu^{2+}] attributes to the formation of 2:1 (ligand:metal) complex between **2** and Cu^{2+} (ESI, Fig. S21, right). Due to the formation of this type of complex the structure becomes very rigid, this may be the reason for this enormous fluorescence enhancement of **2** with addition of Cu^{2+}. The binding constants for both the complexes have been calculated using modified Benesi–Hildebrand (B–H) [28] equation. The binding constant for [**1**-Cu^{2+}] is 5.2 x 10^5 $M^{-1/2}$ and for [**2**-Cu^{2+}] is 1 x 10^4 $M^{-1/2}$ (ESI, Fig. S22).

3.7. Theoretical calculation

To realize the nature of bonding interaction of **1** and **2** with Cu^{2+} as well as to visualise the most probable structures of the complexes, structural calculations have been preformed for **1** and **2** using Gaussian 03 software with B3LYP- hybride functional and 6-31G(*d,p*) basis set and for **1**-

Cu^{2+} and **2**-Cu^{2+} B3LYP with a LANL2DZ relativistic pseudopotential basis set at Density Functional Theory (DFT) level [29].The optimized geometries of **1** shows that pyrene and naphthalene ring are not in same plane, tiled by an angle 62.23^0. By complexation with Cu^{2+} the angle between the pyrene and naphthalene planes reduces to 10.12^0 (Fig. 6, ESI Table S3). It has

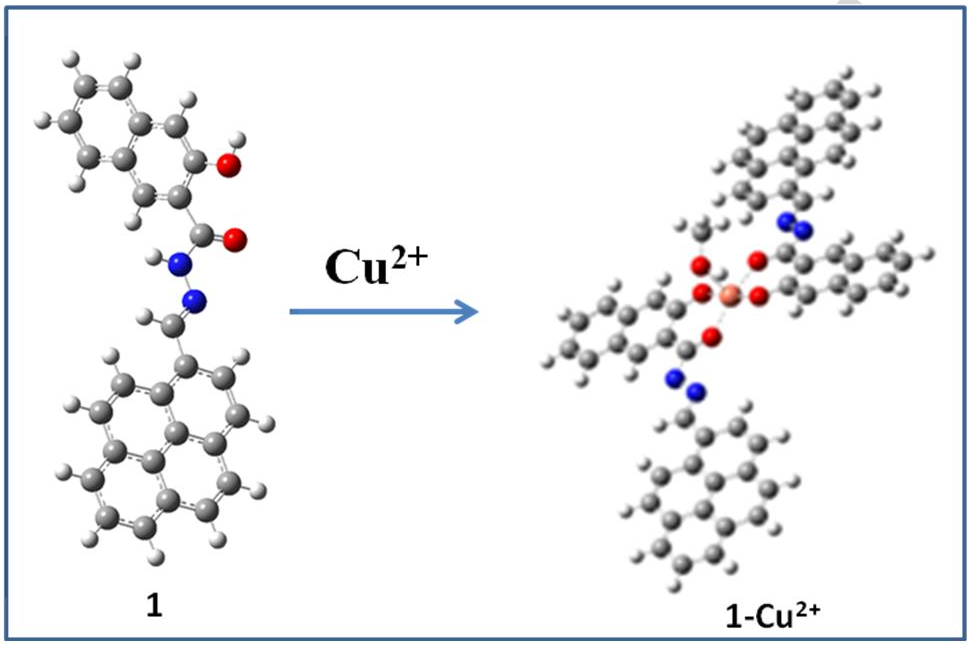

Fig. 6. B3LYP optimized structure of **1** and **1** –Cu^{2+} complex.

been found that the complex formed between **1** and Cu^{2+} is square pyramidal in nature where four coordination sites of the central ion has been filled by two oxygens of two aromatic –OH groups and two oxygens from –CONH-groups of two ligands. The fifth cordination site is fullfilled by methanol. In case of compound **2** , it forms a square planer geometry with Cu^{2+} where four donor atoms are two amidic oxygen and two immine nitrogen from each ligand (Fig.7, ESI Table S4). The angle between the pyrene and naphthalene planes in the **2**-Cu^{2+}complex remains almost unchanged from its free form. The spatial distributions and orbital

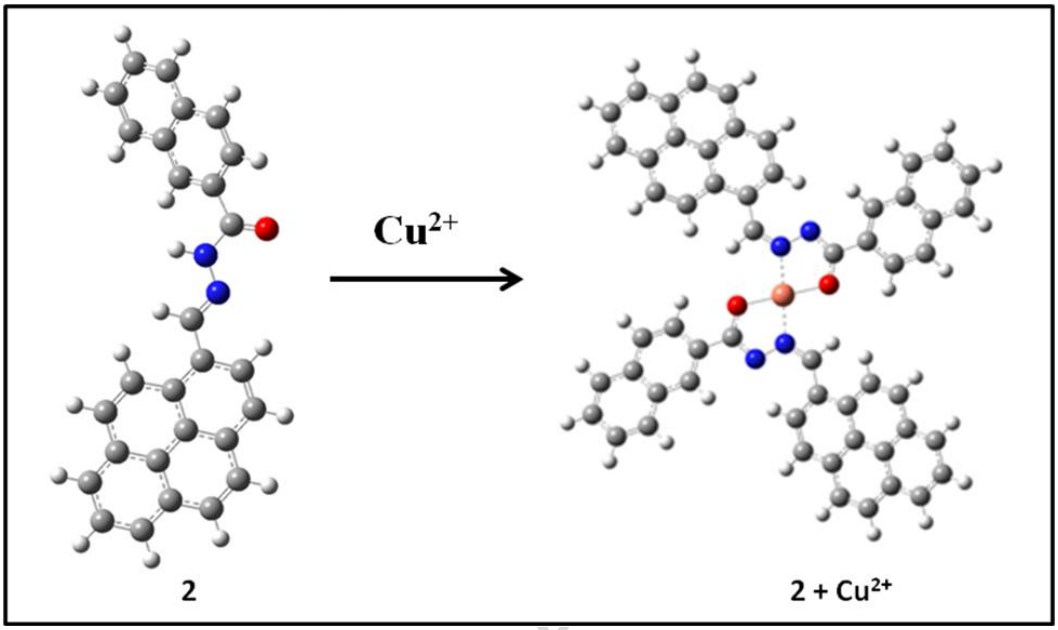

Fig. 7. B3LYP optimized structure of **2** and **2** –Cu^{2+} complex.

energies of the HOMO and LUMO of **1, 2, 1**-Cu^{2+} and **2**-Cu^{2+} complex have been also determined. The energy gaps between HOMO and LUMO in the compound **1** and the **1**-Cu^{2+}complex are 3.29 eV and 1.08 eV respectively and for **2** and **2**-Cu^{2+} are 3.2 eV and 2.4 eV respectively (ESI, Fig. S23 and Fig. S24).

3.8. Kinetic study of 1-Cu^{2+} and 2-Cu^{2+}association

The kinetics of metal ligand interaction has some crucial diagnostic significance.[30] The kinetics of the **1**-Cu^{2+} association reaction has been studied by monitoring the UV-Vis spectral changes of **1** at 485 nm (λ_{abs}) and **2**-Cu^{2+} association reaction has been monitored by the fluorescence enhancement of **2** at 422 nm (λ_{em}) upon interaction with Cu^{2+} at 25 ^{o}C (ESI, Fig. S25 and Fig.

S26). Both the absorbance and fluorescence trace has been fitted by an exponential rise function according to a pseudo-first order kinetics model where the concentration of Cu^{2+} (4 equiv.) in the solution under investigation is significantly larger than that of the ligands (0.2μM). It has been found that the association kinetics of **1** with Cu^{2+} obtained from absorbance data is found to be characterized by a rate constant (k_a) =3.4 ×10^{-2} s^{-1} and the rate constant (k_b) for the association kinetics of **2** and Cu^{2+} is 1.2 × 10^{-2} at 298 K. Furthermore, the association reaction between **1** and Cu^{2+} has been completed within 6 minutes, whereas the association reaction between **2** and Cu^{2+} takes 5 minutes. Therefore, these systems can be used for real-time tracking of Cu^{2+} ion.

3.9.The preliminary Applications of compound 1 and 2

3.9.1. Visual colour changes on test papers

The practical applicability of both the compounds **1** and **2** as Cu^{2+} sensor have been investigated. To explore this, we have prepared test kits by coating a test paper (Whatman-40) with aqueous methanolic solution (v/v 3:7) of **1** and **2** (1× 10^{-4} M) and then dried in air. For the detection of Cu^{2+} by **1**, the aqueous solution of Cu^{2+} (1× 10^{-4} M) have been added on to the test paper and dried in hot air. Interestingly, the spot shows a light brown color (ESI, Fig. S27). In case of compound **2** after the addition of Cu^{2+} the spot on the test kit exhibits bluish white color under UV light (ESI, Fig. S28). So both the compound can be used as Cu^{2+} sensors in solid state also.

3.9.2. Biological Studies of 2 in Presence of Cu^{2+}

As compound **2** detects Cu^{2+} ion by emission intensity enhancement in the visible region in semi-aqueous medium, it can be used for its practical bio-imaging application. For this purpose cytotoxicity of a particular compound is a very important parameter. In order to test cytotoxicity of **2**, we have performed MTT assay in RAW 264.7 cells treated with various concentrations (0 –

0.000037M) of compound **2** for up to 24 hrs. Fig. S29 shows the percentage of cell survivability of compound **2** in different concentrations. This study provides us enthusiastic information regarding its cellular application at the indicated dose and time of incubation without much concern about its cytotoxicity. The viability of RAW 264.7 cells has not been influenced by the amount of solvent (5% DMSO) which has been used for the experiment [30]. Fluorescence microscopic studies revealed that compound **2** shows negligible fluorescence in RAW 264.7 cells (Fig. 8). Upon incubation with Cu^{2+} followed by compound **2**, fluorescence enhancement has

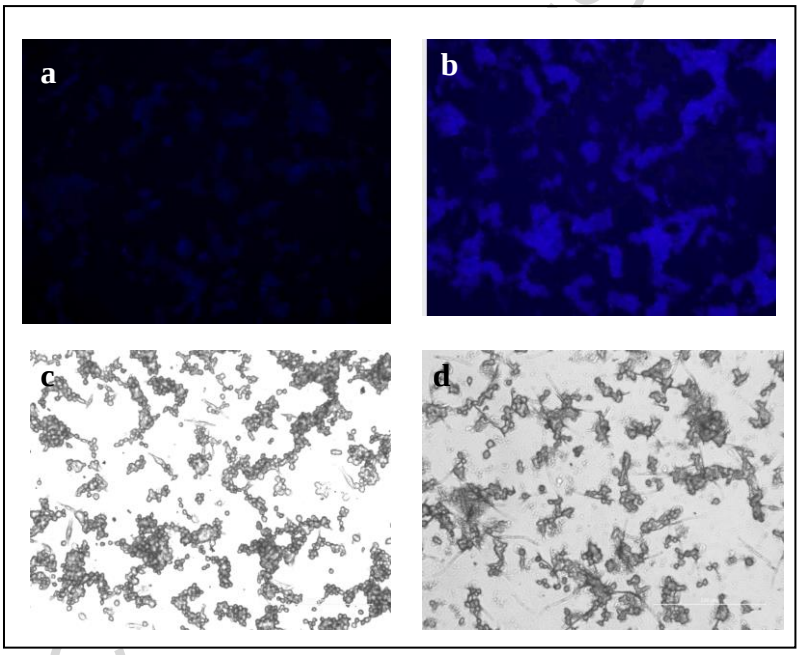

Fig. 8. Fluorescence microscopic images of **2** in RAW 264.7 pretreated with Cu^{2+} : (a) **2** ($1x10^{-6}$ M), (b) **2** ($1x\ 10^{-6}$ M) in presence of Cu^{2+} ($1x10^{-4}$ M) (c) Bright field image of **2** ($1x\ 10^{-6}$ M), (d) Bright field image of **2** ($1x10^{-6}$ M)in presence of Cu^{2+}($1x10^{-4}$ M).

been observed inside RAW 264.7 cells indicating the interaction of **2** with Cu^{2+} which

collaborates well with the solution phase study. The Fluorescence microscopic analysis suggests that compound **2** can sense intracellular Cu^{2+} by readily crossing the membrane barrier of the RAW 264.7 cells. Thus, **2** can be a suitable fluorescence chemosensor for Cu^{2+} detection in biological systems.

4. Conclusions

In summary, two amido-schiff bases (compound **1** and **2**) have been synthesized having a common structural unit, only differs by a –OH group. Both the compounds **1**and **2** can detect Cu^{2+} ion selectively in semi-aqueous medium but the output signals are distinctly different, i.e. compound **1** detects Cu^{2+} by naked-eye color change where as compound **2** detects Cu^{2+} by fluorescence enhancement. Experimental results insist that different mode of binding between the compounds and Cu^{2+} is responsible for this phenomenon. Test strips based on both **1** and **2** have been fabricated, which act as a convenient and efficient Cu^{2+} test kit. The biological application of **2** has been evaluated in RAW 264.7 cell and it shows good membrane permeability for the detection of Cu^{2+}. On the basis of the above results, it can be said that both the compound **1** and **2** can serve as efficient sensor for Cu^{2+} in semi-aqueous medium and we believe that this current discussion, the effect of mode of binding on signaling property of the ligands will offer an important guidance for the interactions of biologically important ions with receptor molecules.

Acknowledgements

SG and AG acknowledge UGC and CSIR, India for senior research fellowships. NG likes to acknowledge CAS-V, UGC and DST-FIST, India for instrumental assistance.

References

1. P. L. Malvankar and V. M. Shinde, Ion-pair extraction and determination of copper (II) and zinc(II) in environmental and pharmaceutical samples, Analyst., 1991,116, 1081-1084.

2. S. Hu, P. Furst and D. Hamer, The DNA and Cu binding functions of ACE1 are interdigitated within a single domain, *New Biol*. 1990, **2**, 544-555.

3. E. Gaggelli, H. Kozlowski, D. Valensin and G. Valensin, Copper Homeostasis and Neurodegenerative Disorders (Alzheimer's, Prion, and Parkinson's Diseases and Amyotrophic Lateral Sclerosis)*Chem Rev*., 2006, **106**, 1995-2044.

4. Y.H. Hung, A.I. Bush and R.A. Cherny, Copper in the brain and Alzheimer's disease ,*J. Biol. Inorg. Chem*., 2010, **15**, 61-76.

5. J.Y. Uriu-Adams and C.L. Keen, Copper, oxidative stress, and human health *Mol. Aspects Med.*, 2005, **26**, 268-298.

6. A.C. Liu, D.C. Chen, C.C. Lin, H.H. Chou and C.H. Chen, Application of Cysteine Monolayers for Electrochemical Determination of Sub-ppb Copper(II), *Anal. Chem*., 1999, 71, 1549-1552.

7. K. Cui, X.M. Lu, W. Cui, J. Wu, X.M. Chen and Q.H. Lu, Fluorescent nanoparticles assembled from a poly(ionic liquid) for selective sensing of copper ions, *Chem. Commun*., 2010, **47**, 920-922.

8. Y.Q. Dong, R.X. Wang, G.L. Li, Y.W. Chi and G.N. Chen, Polyamine-Functionalized Carbon Quantum Dots as Fluorescent Probes for Selective and Sensitive Detection of Copper Ions, *Anal. Chem*., 2012, **84**, 6220-6224.

9. T.T. Lou, L.X. Chen, Z.P. Chen, Y.Q. Wang, L. Chen and J.H. Li, Colorimetric Detection of Trace Copper Ions Based on Catalytic Leaching of Silver-Coated Gold Nanoparticles, *ACS Appl. Mater. Interface.*, 2011, **3**, 4215-4220.

10. B.C. Yin, B.C. Ye, W.H. Tan, H. Wang and C.C. Xie, An Allosteric Dual-DNAzyme Unimolecular Probe for Colorimetric Detection of Copper(II)*J. Am. Chem. Soc.*, 2009, **131**, 14624-14625.

11. T.W. Lin and S.D. Huang, Direct and Simultaneous Determination of Copper, Chromium, Aluminum, and Manganese in Urine with a Multielement Graphite Furnace Atomic Absorption Spectrometer, *Anal. Chem.*, 2001, **73**, 4319-4325.

12. A.P.S. Gonzáles, M.A. Firmino, C.S. Nomura, F.R.P. Rocha, P.V. Oliveira and I. Gaubeur, Peat as a natural solid-phase for copper preconcentration and determination in a multicommuted flow system coupled to flame atomic absorption spectrometry,*Anal. Chim. Acta.*, 2009, **636**, 198-204.

13. N. Mergua and V. K. Gupta, A novel colorimetric detection probe for copper(II) ions based on a Schiff base *Sensor, Actuat B-Chem.*, 2015, **210**, 408-471.

14. L.-H. Jin and C.-S. Han, Ultrasensitive and Selective Fluorimetric Detection of Copper Ions Using Thiosulfate-Involved Quantum Dots, *Anal. Chem.*, 2014, **86**, 7209-7213.

15. A. Ganguly, B. K. Paul, S. Ghosh, S. Kar and and N. Guchhait, Selective fluorescence sensing of Cu(II) and Zn(II) using a new Schiff base-derived model compound: naked eye detection and spectral deciphering of the mechanism of sensory action ,*Analyst*, 2013, 138, 6532-6541.

16. G. J. Park, G. R. You, Y. W. Choi and Cheal Kim, A naked-eye chemosensor for simultaneous detection of iron and copper ions and its copper complex for colorimetric/fluorescent sensing of cyanide *Sensor Actuat B-Chem.*, 2016, **229**,257-271.

17. L. Zeng , E. W. Miller, A. Pralle , E.Y. Isacoff and C. J. Chang, A Selective Turn-On Fluorescent Sensor for Imaging Copper in Living Cells, *J. Am. Chem. Soc.*, 2006, **128**, 10–11

18. Y. Qian, L. Cao, C. Jia, P. O. Boamah, Q. Yang, C. Liu, Y. Huangd and Qi Zhang, A highly selective chemosensor for naked-eye sensing of nanomolar Cu(II) in an aqueous medium*RSC Adv.*, 2015,**5**, 77965-77972.

19. L. Feng, H. Li, Y. Lv and Y. Guan, Colorimetric and "turn-on" fluorescent determination of Cu2+ ions based on rhodamine–quinoline derivative, *Analyst*, 2012, **137**, 5829–5833

20. P. Patrycja, S. Janusz, J. Anna, T. Bartosz, N. Wojciech and H. Maciej, Synthesis, structural characterization and spectroscopy studies of new oxovanadium(IV, V) complexes with hydrazone ligands, Polyhedron, 2015, 87, 226–232.

21. D. Prasad, A. Aamir, D. Jyoti, S. K. Venkateswara, K. M. Ejazuddin, K. Madhukar, P. Subhash and S. Fazlul, Anticancer phytochemical analogs 37: Synthesis, characterization, molecular docking and cytotoxicity of novel plumbagin hydrazones against breast cancer cells, Bioorganic & Medicinal Chemistry Lett., 2014, 24, 2900-2904.

22. B. K. Paul and N. Guchhait, A spectral deciphering of the binding interaction of an intramolecular charge transfer fluorescence probe with a cationic protein: thermodynamic analysis of the binding phenomenon combined with blind docking study, Photochem. Photobiol. Sci., 2011, 10, 980-991.

23. S. Dalapati, S. Jana, Md. A. Alam, N. Guchhait, Multifunctional fluorescent probe selective for Cu(II) and Fe(III) with dual-mode of binding approach, Sensor and Actuators B,2011, 160,1106-1111.

24. S. Ressalan, C. S. P. Iyer, Absorption and fluorescence spectroscopy of 3-hydroxy-3-phenyl-1-o-carboxyphenyltriazene and its copper (II), nickel (II) and zinc (II) complexes: a novel fluorescence sensor, J. Lumin. 2005, 111, 121-129.

25. M.-Y. Choi, M. C.-W. Chan, S. Zhang, K.-K. Cheung, C.-M. Che, K.-Y. Wong, MLCT and LMCT Transitions in Acetylide Complexes. Structural, Spectroscopic, and Redox Properties of Ruthenium(II) and -(III) Bis(ó-arylacetylide) Complexes Supported by a Tetradentate Macrocyclic Tertiary Amine Ligand, Organometallics, 1999.18, 2074-2080.

26. L. S. Villata, E. Wolcan, M. R. Feliz, A. L. Capparelli, Competition between Intraligand Triplet Excited State and LMCT on the Thermal Quenching in â-Diketonate Complexes of Europium(III), J. Phys. Chem. A, 1999,103, 5661-5666.

27. (a)S. Ghosh, A. Ganguly, M. R. Uddin, S. Mandal, M. A. Alam and N. Guchhait, Dual mode selective chemosensor for copper and fluoride ions: a fluorometric, colorimetric and theoretical investigation, Dalton Trans., 2016,45, 11042-11051. (b) H.-F. Wang, S.-P. Wu, A pyrene-based highly selective turn-on fluorescent sensor for copper(II) ions and its application in living cell imaging, Sensor and Actuators B 181 (2013) 743-748.

28. A. Samantaa, N. Guchhait , S. C. Bhattacharya, A simple but highly selective and sensitive fluorescence reporter for toxic Cd^{II} ion via excimer formation, Chemical Physics Letters 612 (2014) 251–255.

29. M.J. Frisch, G.W. Trucks, H.B. Schlegel, G.E. Scuseria, M.A. Robb, J.R. Cheeseman, G. Scalmani, V. Barone, B. Mennucci, G.A. Petersson, H. Nakatsuji, M. Caricato, X. Li, H.P.

Hratchian, A.F. Izmaylov, J. Bloino, G. Zheng, J.L. Sonnenberg, M. Hada, M. Ehara, K. Toyota, R. Fukuda, J. Hasegawa, M. Ishida, T. Nakajima, Y. Honda, O. Kitao, H. Nakai, T. Vreven, J.A. Montgomery, J.E. Peralta, F. Ogliaro, M. Bearpark, J.J. Heyd, E. Brothers, K.N. Kudin, V.N. Staroverov, R. Kobayashi, J. Normand, K. Raghavachari, A. Rendell, J.C. Burant, S.S. Iyengar, J. Tomasi, M. Cossi, N. Rega, J.M. Millam, M. Klene, J.E. Knox, J.B. Cross, V. Bakken, C. Adamo, J., Jaramillo, R., Gomperts, R.E. Stratmann, O. Yazyev, A.J. Austin, R. Cammi, C. Pomelli, J.W. Ochterski, R.L. Martin, K. Morokuma, V.G. Zakrzewski, G.A. Voth, P. Salvador, J.J. Dannenberg, S. Dapprich, A.D. Daniels, Ö. Farkas, J.B. Foresman, J.V. Ortiz, J. Cioslowski, D.J. Fox, Gaussian 09, Revision B.01, Inc., Wallingford, CT, 2009. 30.

30. G. G. Hammes and S. A. Leviso, A Kinetic Investigation of the Interaction of Adenosine-5′-triphosphatew ith Divalent Metal Ions, Biochemistry,1964, 3, 1504-1506.

Binding mode dependent signaling for the detection of Cu^{2+}: An experimental and theoretical approach with practical applications

Soumen Ghosh[a], Md. Mehebub Ali Khan[b], Aniruddha Ganguly[a], Abdulla Al Masum[b], Md. Akhtarul Alam[b*] and Nikhil Guchhait[a*]

Graphical abstract

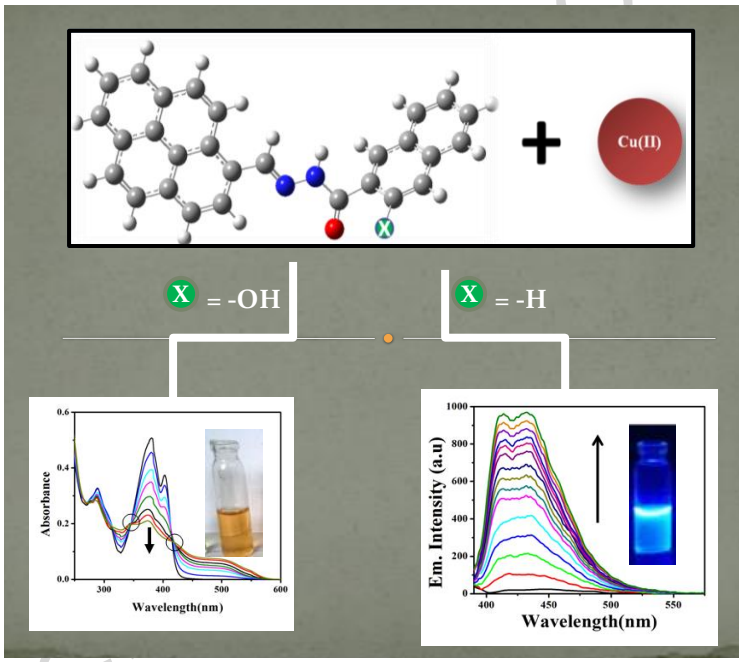

Highlight Points:

►Newly designed compounds selective sensor for Cu^{2+} ion in semi-aqueous medium.

► Compound **1** detects Cu^{2+} by naked-eye color change where as compound **2** detects Cu^{2+} by fluorescence enhancement.

►The detection limit of compound **1** towards Cu^{2+} is in micromolar region whereas the compound **2** detects Cu^{2+} in nano-molar region.

►Compound **2** exhibits good membrane permeability for the detection of Cu^{2+}.